Chinese Journal of Chemical Engineering 58 (2023) 306–314

Contents lists available at ScienceDirect

Chinese Journal of Chemical Engineering

journal homepage: www.elsevier.com/locate/CJChE

Full Length Article

Formation of the structure-II gas hydrate from low-concentration propane mixed with methane

Sanya Du [1,2,#], Xiaomin Han [1,#], Wenjiu Cai [3,4,#], Jinlong Zhu [5,6], Xiaobai Ma [7], Songbai Han [8], Dongfeng Chen [7], Yusheng Zhao [5,6], Hui Li [1,*], Hailong Lu [4,*], Xiaohui Yu [2,9,*]

[1] Beijing Advanced Innovation Center for Soft Matter Science and Engineering, Beijing University of Chemical Technology, Beijing 100029, China
[2] National Laboratory for Condensed Matter Physics, Institute of Physics, Chinese Academy of Sciences, Beijing 100190, China
[3] College of Engineering, Peking University, Beijing 100871, China
[4] Beijing International Center for Gas Hydrate, School of Earth and Space Sciences, Peking University, Beijing 100871, China
[5] Department of Physics, Southern University of Science and Technology (SUSTech), Shenzhen 518055, China
[6] Southern Marine Science and Engineering Guangdong Laboratory (Guangzhou), Guangzhou 511458, China
[7] Department of Nuclear Physics, China Institute of Atomic Energy, Beijing 102413, China
[8] Academy for Advanced Interdisciplinary Studies, Southern University of Science and Technology (SUSTech), Shenzhen 518055, China
[9] Songshan Lake Materials Laboratory, Dongguan 523808, China

ARTICLE INFO

Article history:
Received 6 April 2022
Received in revised form 3 October 2022
Accepted 7 October 2022
Available online 11 November 2022

Keywords:
Multiple guest molecules
Clathrates
Neutron powder diffraction
Structural transformation
Molecular mechanism

ABSTRACT

It has been recognized that a small amount of propane mixed with methane can change greatly in not only the thermodynamics but also the structural properties of gas hydrate. However, its mechanism is still not well understood yet. In this research, structure-II (sII) hydrate is synthesized using a methane-propane gas mixture with an initial mole ratio of 99:1, and it is found that large ($5^{12}6^4$) cages are co-occupied by multiple gases based on the rigid structure analysis of neutron diffraction data. The first principles calculation and molecular dynamics simulation are conducted to uncover the molecular mechanism for sII methane-propane hydrate formation, revealing that the presence of propane inhibits the formation of structure-I (sI) hydrate but promotes sII hydrate formation. The results help to understand the accumulation mechanism of natural gas hydrate and benefit to optimize the condition for gas storage and transportation in hydrate form.

1. Introduction

Natural gas hydrate (NGH) is a kind of non-stoichiometric crystalline material, in which hydrogen-bonded water molecules form cages to host guest gas molecules [1]. NGHs have been found in permafrost and sediments on continental slope worldwide. It is estimated that the global carbon reserve of methane in NGH is over all other discovered oil and gas together [2,3], indicative of its potential to serve as an energy resource in the future. Because of its high energy density [4] (~170 volume gas per volume hydrate), gas hydrate can also be used as a medium for natural gas storage and transportation. However, due to the complexity of local condition (such as pore sediment type, water salinity and interaction between guest molecules and ions) [5–8] and the fragile stability of hydrate [1,9], it is still difficult in developing and utilizing hydrates safely and effectively with current technologies. As gas hydrate is stable only under relatively high pressure and low temperature, optimized gas transportation condition in hydrate form would be also beneficial to cost reduction. Therefore, a better understanding of the formation mechanism and thermodynamic properties of NGHs is indispensable.

NGHs inevitably contain certain amounts of heavy hydrocarbons, such as ethane and propane. Compared with pure methane hydrate, the properties of mixed gas hydrate are more complex [10–17]. It is well-known that pure methane hydrate is with the structure of structure-I (sI). However, the addition of a small amount of ethane will lead to the transformation of hydrate structure from sI to structure-II (sII), as recognized by both theoretical studies and experimental investigations [10,11]. In addition to ethane in natural gas, propane as a common heavier hydrocarbon gas, can also affect the thermodynamic and kinetic properties of mixed-gas hydrate. It is found that, even a small amount of

* Corresponding authors.
E-mail addresses: hli@buct.edu.cn (H. Li), hlu@pku.edu.cn (H. Lu), yuxh@iphy.ac.cn (X. Yu).
# These authors contributed equally to this work.

https://doi.org/10.1016/j.cjche.2022.10.014
1004-9541/

propane mixed with methane the hydrate structure formed will not be sI but sII, and the hydrate will be much more stable, indicating that propane can serve as a promoter and stabilizer of gas hydrate [12,13]. The inclusion of 3%–5% propane in methane can improve the formation kinetics of mixed gas hydrate. Propane enrichment was also found in the hydrate formed from a methane-propane gas mixture, revealing the preferential enclathration of propane into sII hydrates [18]. Although it has been recognized that minor amount of propane in natural gas is with a profound impact on the thermodynamic and kinetic properties of NGH, the mechanism of mixed gas hydrate formation process is still not well understood on the molecular scale. As the result, further investigations are needed to elucidate the molecular mechanism of hydrate formation from mixed minor propane and methane.

However, it is difficult to study mixed gas hydrate with natural samples due to the challenge in natural sample recovery. In such a situation, synthesizing hydrate, with a gas composition simulating natural hydrates, is a widely adopted strategy. The fact that methane-propane gas mixture is one of the simpler systems makes it an appealing model system to study gas hydrate formation.

To understand the formation mechanism of sII hydrate on the molecular scale, both experimental investigation and molecular simulation studies are conducted in this study. The gas hydrate sample is synthesized by the reaction of powdered ice with a methane-propane gas mixture, and the atomistic structure of the sample is determined based on the results of high-resolution neutron powder diffraction (NPD) experiments. The density functional theory (DFT) calculations and molecular dynamics (MD) simulations are also carried out to specify the molecular mechanism of sII hydrate formation from a mixed methane-propane gas.

2. Experimental and Simulation Methods

2.1. Synthesis of structure-II (sII) hydrate

The experimental apparatus used for sII hydrate synthesis is shown in Fig. 1. The sample is synthesized with ~1.4 g of powdered ice prepared by pulverizing the deuterium water (D_2O; Aldrich; 99.9% D) frozen in liquid nitrogen, as shown in Fig. 1(a). In this way, incoherent scattering caused by hydrogen and preferred orientation could be mostly avoided. Then, the D_2O ice powder is loaded into an aluminum cell, which is placed and sealed in a pre-cooled high-pressure reactor (250 ml), as shown in Fig. 1(b) and (c). Subsequently, the sealed reactor is flushed with feed gas (methane-propane gas mixture) four times to exhaust the air before the system is pressured to the desired initial pressure (~8 MPa) at 268.15 K, as shown in Fig. 1(d). The feed gas is obtained from Beijing AP BAIF Gases Industry Co., Ltd. with weighing method, with a gas component of 99% (mol) methane and 1% (mol) propane. After about 10 days, the synthesized methane-propane hydrate is ready for neutron diffraction when no further obvious pressure drop is observed. The aluminum cell is taken out from the reactor and sealed again under liquid nitrogen condition, as shown in Fig. 1(e) and (f). Finally, it is pressured with feed gas (~8 MPa) and stored in the fresh zone of a refrigerator (273.15–275.15 K) before measurement. It should be noted that because deuterium is easily replaced by hydrogen in air, the exposure time of ice or hydrate has to be minimized.

2.2. Determination of the pressure–temperature (P-T) equilibrium condition of hydrate

To evaluate the stability of the synthesized methane-propane deuterated hydrate, the hydrate-liquid-vapor (HLV) equilibria of the methane hydrate and methane-propane deuterated hydrate are determined. The methane hydrate is synthesized with ice powder and methane gas (99.9%). The methane-propane deuterated hydrate is synthesized from deuterated ice powder (99.9% D) and a gas mixture with an initial gas composition of 99% (mol) methane and 1% (mol) propane. The hydrate is first synthesized at a high pressure and circulating temperature (268.15–277.15 K) in the high-pressure reactor shown in Fig. 1, which is equipped with two temperature sensors and a pressure transducer (Brighty Instrument Co., Ltd.) with a range of 0–20 MPa and an accuracy of ~0.05 MPa. When the pressure essentially keeps constant, the

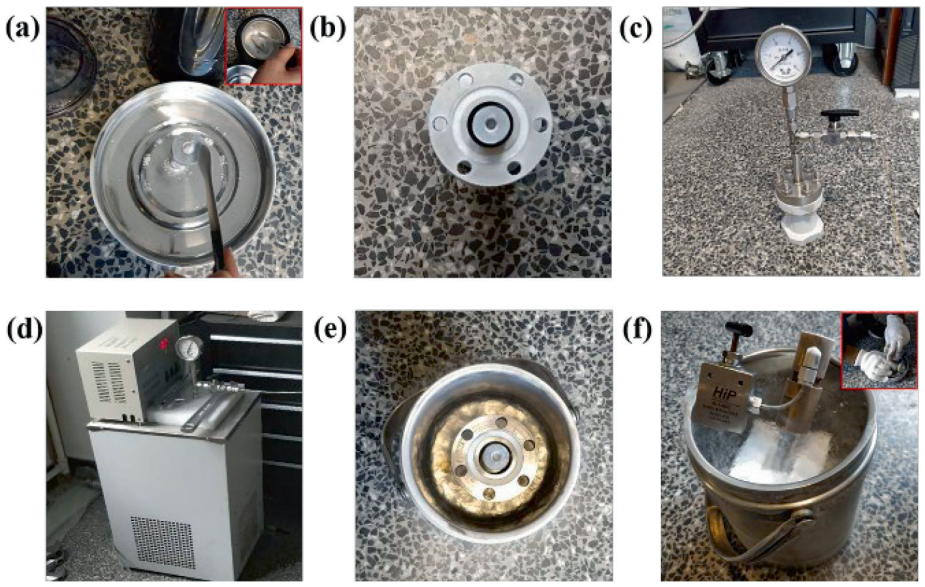

Fig. 1. Methane-propane hydrate synthesis in a stainless-steel reactor for NPD measurements. (a) D_2O ice is pulverized with a grinder after being frozen in liquid nitrogen. (b) D_2O powder is added into an aluminum cell, which is then placed in a pre-cooled high-pressure reactor. (c) The aluminum cell is sealed in the reactor. (d) The reactor is placed in a circulator bath, and then flushed with methane-propane gas mixture four times. Finally, it is pressurized to 8 MPa. After several days, methane-propane hydrate forms. (e) The reactor is opened under liquid nitrogen condition and the aluminum cell, which contains hydrate, is removed. (f) The hydrate is sealed in the aluminum cell, which is placed in liquid nitrogen. The cell is then transferred into the fresh zone of a refrigerator for storage before the NPD experiment.

hydrate synthesis is considered finished. At this point, the gas in the reactor is released stepwise (0.05 MPa each time) at constant temperature until the observation of internal pressure recovery after gas release, indicating the dissociation of gas hydrate. The dissociation will continue until there is barely no change in system pressure for over 6 h, at which point a new equilibrium is considered to have been reached. The pressure and temperature values are recorded to obtain the equilibrium condition under the corresponding gas phase composition. Then, the previous steps are repeated for more equilibrium points.

2.3. Neutron powder diffraction (NPD) experiment

The structure of the mixed methane-propane hydrate is investigated using high-resolution NPD at China Institute of Atomic Energy. Fig. 2(a) and (b) shows a schematic layout of the high-resolution NPD and the experimental setup for neutron diffraction of hydrate at low temperature and high pressure, respectively. The scattering covers a range from 7° to 146° (corresponding d-space range), for the determination of lattice parameters and configuration of atomic positions of the hydrate studied. Based on the detector geometry and refinement using multi-bank data, the structure type, structural parameters, and refinement details of the methane-propane mixed gas hydrate are obtained, including the cage occupancies of methane and propane molecules.

2.4. Binding energy calculation and molecular dynamics (MD) simulation

The first principles calculations, in which the interactions between molecules are accurately described, are carried out in the framework of DFT using the CP2K [19] package. The Becke-Lee-Yang-Parr (BLYP) functional [20,21] combined with the Grimme dispersion correction (DFT-D3) [22], DZVP basis set and the Goedecker-Teter-Hutter (GTH) norm-conserved pseudopotentials [23,24] are implemented to calculate the interactions between different kinds of guest molecules and large and small water cages. A cutoff energy of 3.8×10^3 eV is applied for all calculation processes. For each simulated system, a methane molecule or a propane molecule is placed in the large ($5^{12}6^2$ and $5^{12}6^4$) and small (5^{12}) cages in the primitive cells of sI or sII hydrate for simulations. The strength of interaction is expressed by the binding energy ($E_{binding}$), and the calculation formula is as following:

$$E_{binding} = E_{total} - E_{guest} - E_{cage}$$

where E_{total} represents the total energy of the system, E_{guest} represents the energy of the guest molecules, and E_{cage} represents the total energy of hydrate with empty cages.

The MD simulations are performed using the GROMACS package [25]. The rigid (TIP4P-Ew) model [26] and the optimized potentials for liquid simulations all-atom (OPLS-AA) forcefield [27] are applied to describe the water and hydrocarbon molecules, respectively. The Lorentz-Berthelot mixing rule is employed to calculate the Lennard-Jones potentials between different molecules. Short-range van der Waals interactions are truncated at 1 nm, and the particles-mesh Ewald algorithm with a Fourier grid spacing of 0.12 nm is used to calculate the long-range electrostatic interactions. The MD simulations are conducted in both the constant-volume-and-temperature (NVT) and the constant-pressure-and-temperature (NPT) ensembles. The Nose-Hoover thermostat [28] is employed to control the temperature of the simulation system with a time constant of 2 fs, and the anisotropic Parrinello-Rahman barostat [29] is employed to control the pressure of the simulation system with a time constant of 4 fs and a compression coefficient of 4.58×10^{-4} MPa^{-1}. The time step in all simulation processes is 1 fs.

A two-phase equilibrium model is employed for the initial atomic configuration of simulation to reduce thermodynamic hysteresis, with half of the hydrate and half of the water/methane-propane liquid solution in contact with each other. To generate reasonable hydrate/solution configuration, we build up the boxes of perfect sI [30] and sII [31] hydrates, in which the methane: propane ratios are 1:0, 11:1 and 2:1. The initial simulation systems containing $9 \times 2 \times 2$ and $6 \times 2 \times 2$ unit cells of sI and sII hydrates, respectively, are called System sI-1, System sI-2, System sI-3, System sII-1, System sII-2, and System sII-3. With the atomic positions of 1/9 of System sI-1, System sI-2, and System sI-3, and 1/6 of System sII-1, System sII-2, and System sII-3 being kept frozen along the *x* direction, the rest regions of hydrate systems are melted at the temperature of 350 K for 10 ns to ensure no residual structure remained. The obtained hydrate/solution mixed configurations are used as the starting points in MD simulations in the NPT ensemble, and a simulated pressure of 80 MPa, much higher than the experimental pressure, is employed to speed up the simulation processes.

3. Results and Discussion

3.1. Atomistic structure of methane-propane hydrate

Neutron diffraction is an important method for analysing and studying the structure of samples especially in light elements-containing systems. Neutrons have a strong penetration, are sensitive to light elements, and can measure samples with a volume of ~1 cm^3. Therefore, neutron diffraction has obvious advantages in hydrate research systems compared with X-ray diffraction and

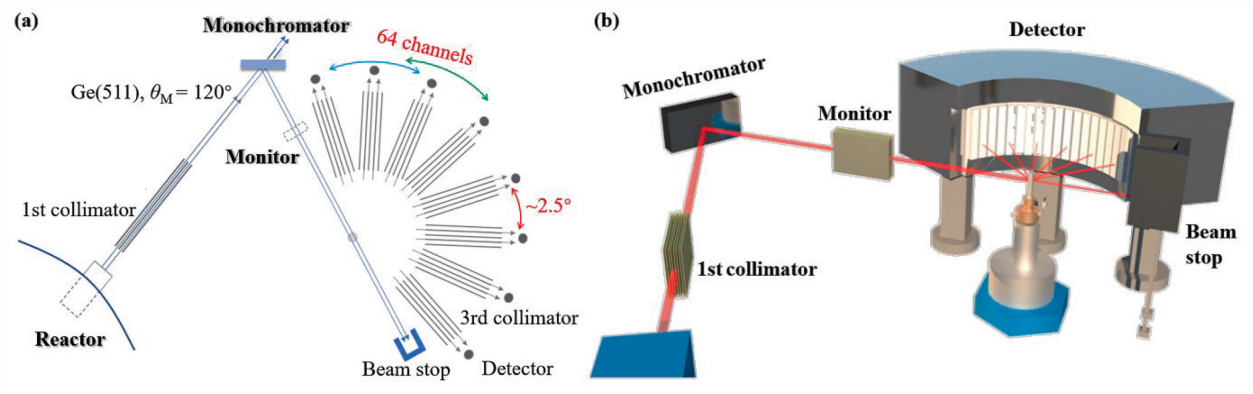

Fig. 2. High-resolution NPD setup at China Institute of Atomic Energy. (a) Schematic layout of the high-resolution NPD. (b) 3D illustration of the experimental facility of neutron diffraction of hydrate.

Raman spectroscopy. Fig. 3(a) shows the neutron diffraction pattern of the synthesized methane-propane hydrate, and it is processed with rietveld refinements using GSAS (general structure analysis system) software. The hydrate is identified with a crystal space group of $Fd\bar{3}m$ with a unit cell parameter of 1.73 nm, known as cubic sII [1]. It means, the framework of this hydrate structure is composed of 5^{12} and $5^{12}6^4$ cages formed by hydrogen-bonded D_2O molecules.

Studies have shown that the addition of only 1% (mol) propane to methane is sufficient to transform the structure of hydrate from sI to sII [1,32]. In this work, we synthesize hydrate from the ice powder and a mixed gas initially containing 1% (mol) propane, which is enough for the formation of sII hydrate. The hydrate formation will first happen around ice surfaces, where the amounts of formed hydrates are relatively limited and the fractionation in gas composition is also limited. According to the experimental conditions (the amount of ice powder, the composition and pressure of the mixed gas, the volume of the cell and the reactor), even if the ice powder is completely reacted, propane in the mixed gas should be still remained. Actually, the ice powder is not completely converted, and propane molecules would not have been completely consumed at the end of the experiment. Consequently, the formation of sI methane hydrate after the fully consumption of propane as in Uchida's work [33] does not occur in this article and only sII hydrate is formed. There are also studies shown that the hydrate structure formed by a methane-propane gas mixture with a ratio of 98:2 can transform from single phase (sII) to multiphase (sI and sII) if the temperature is lowered to a certain level under constant pressure [34]. When the experimental conditions are close or in the stable region of sI methane hydrate, sI hydrate may be formed. Even so, as the sII hydrate is more thermodynamically stable, the employment of circulating temperature during the hydrate formation may lead to the gradual transformation of sI hydrate into the sII hydrate, which can explain the only formation of sII hydrate. It can also be learned from refinement (Fig. 3 (a)) that the ratio of the synthesized sII hydrate to the remaining ice is approximately 0.4 (29:71), close to the ratio of the highest peak intensities of the two phases (0.37). Accordingly, the value is reasonable.

The synthesized methane-propane hydrate in our work has the same sII-hydrate structure as the propane hydrate, whose atomic coordinates and gas occupancy have been obtained through neutron diffraction [35]. However, the hydrate in our experiment is synthesized with methane-propane gas mixture. To get its fine structure information, some modifications need to be made based on the known propane hydrate model. Before refinement, the carbon atoms of the methane molecules are added at the centres of the small (S) and large (L) cages, occupying the 16*c* site (1/8, 1/8, 1/8) and the 8*b* site (1/2, 1/2, 1/2), respectively. The position coordinates of the related hydrogen atoms can be obtained from a rigid body model of a methane molecule. In the unit cell of sII hydrates, there are 8 L cages and 16 S cages. The hydrogen and carbon atoms in the propane are all located at 192*i* sites. The filling rate of propane molecules in the L cage is calculated to be 24 (192/8) times the occupancy of C10, whereas the filling rate of methane molecules in L and S cages are consistent with the occupancies of C21 at 8*b* site and C26 at 16*c* site, respectively. Every hydrogen atom of methane is also located at a 192*i* site.

Fig. 3(b) shows the structural model of sII methane-propane hydrate from the Rietveld refinement. Fig. 3(c) shows the methane molecules with full symmetry in S and L cages and propane molecules with full symmetry in L cages in hydrate. The ratios of colours on the balls give an intuitive indication of the atomic occupancies. For example, carbon atoms (purple balls) in propane have a very small percentage of purple, corresponding to the occupancy of 0.0247. The experimental parameters, crystal data, and refinement details for the methane-propane hydrate are listed in Table 1. The results shown in Table 2 indicate that both propane and methane molecules can occupy the L cages, while only methane molecules occupy the S cages. The filling rates of methane and propane molecules in the L cages are 36.38% and 59.28%, respectively, whereas the filling rate of methane molecules in S cages is 72.99%. As seen from the refinement results, the occupancies of carbon atoms are 24 (0.3638/0.0152) times those of the hydrogen atoms in the L cages which are equal to 192/8. Similarly, the occupancies of car-

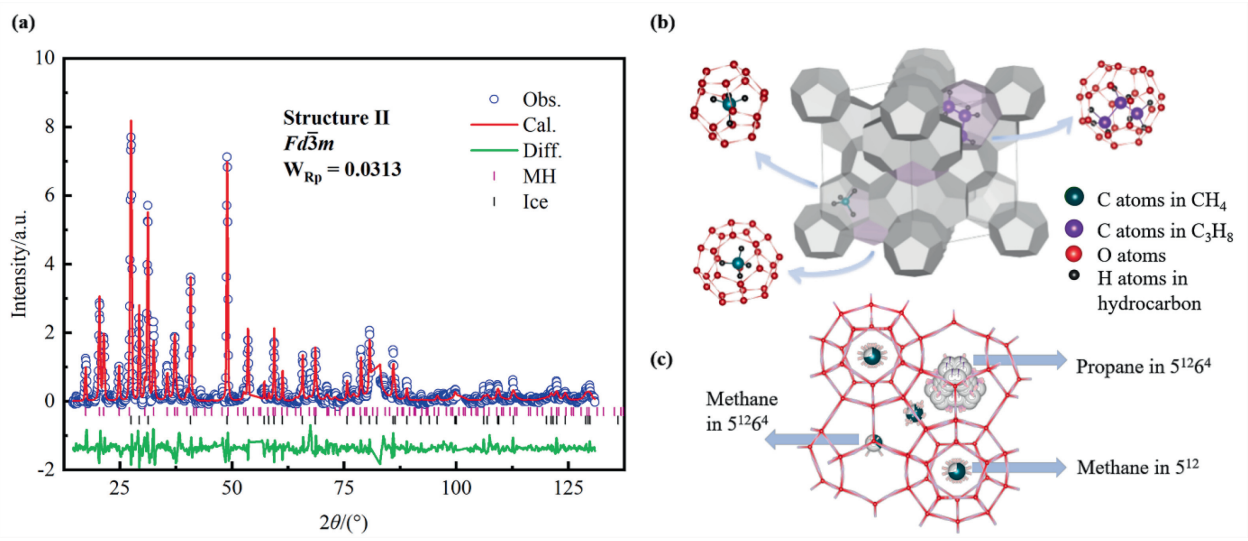

Fig. 3. (a) High-resolution NPD patterns of methane-propane hydrate (synthesized from a methane-propane gas mixture with an initial propane concentration of 1% (mol)). The blue dot solid (Obs.) and red solid (Cal.) lines represent the observed intensity normalized using the incident beam and the pattern calculated using the rietveld method, respectively. The purple and black marks indicate the peak positions of methane-propane hydrate and ice Ih, respectively. The green line (Diff.) under the tick marks is the difference curve between Obs. and Cal. (b) Structural model of methane-propane hydrate. Each cage is formed by water molecules, and the S (5^{12}) and L ($5^{12}6^4$) cages combine to form sII. The vertices of the cages are oxygen atoms, and the deuterium atoms are connected to the oxygen. Methane molecules are located in the centres of the S and L cages, while propane molecules are located only in the centres of the L cages. (c) Propane in sII-L cages and methane in sII-S and sII-L cages with full symmetry, different colour ratios represent different atomic occupancies.

Table 1
Experimental conditions of NPD analysis, crystal parameters and refinement details for the methane-propane mixed gas hydrate

Powder diffraction data collection		Crystal data	
Wavelength/nm	0.1888	Crystal system	Cubic
Scan range 2θ/(°)	7–146	Space group	$Fd\bar{3}m$
Step size 2θ/(°)	0.07	a/nm	1.73
Temperature/K	273.15	Volume/nm^3	5.178
Instrument	HRPD	—	—

Note: wR_p = 0.0313, $R_{(exp)}$ = 0.0224, $R_{(F^{**}2)}$ = 0.1494. *R*-factor represents the difference between experimental and theoretical values, the smaller the value difference is, the better the data quality and credibility are. Among them, the full name of wR_p is weighted-R pattern and refers to weighted graph variance factor; the full name of $R_{(exp)}$ is *R*-expected and refers to expected variance factor; $R_{(F^{**}2)}$ is related to reflection data statistics.

Table 2
Atomic coordinates of methane-propane hydrate from the rietveld refinement of NPD data collected at 273.15 K (space group: $Fd\bar{3}m$; origin at center (3m), at 1/8, 1/8, 1/8 from $\bar{4}3$ m)

Atom	Occupancy	Muit.	*x*	*y*	*z*
O1	1.0000	96 *g*	0.180819	0.180819	0.364076
O2	1.0000	32*e*	0.217219	0.217219	0.217219
O3	1.0000	8*a*	0.125000	0.125000	0.125000
D4	0.5000	192*i*	−0.017781	−0.165085	0.143776
D5	0.5000	96 *g*	0.143819	0.143819	0.363776
D6	0.5000	96 *g*	0.190519	0.190519	0.310776
D7	0.5000	96 *g*	0.206519	0.206519	0.264776
D8	0.5000	32*e*	0.158519	0.158519	0.158519
D9	0.5000	32*e*	0.181519	0.181519	0.181519
C10	0.0247	192*i*	0.398340	0.371817	0.438942
C11	0.0247	192*i*	0.372840	0.441918	0.392642
C12	0.0247	192*i*	0.298240	0.432718	0.349342
H13	0.0247	192*i*	0.450140	0.379517	0.470642
H14	0.0247	192*i*	0.347140	0.359518	0.480642
H15	0.0247	192*i*	0.399140	0.321517	0.399642
H16	0.0247	192*i*	0.369140	0.493518	0.431642
H17	0.0247	192*i*	0.420140	0.455518	0.350642
H18	0.0247	192*i*	0.251140	0.419518	0.391642
H19	0.0247	192*i*	0.303140	0.382518	0.309642
H20	0.0247	192*i*	0.283140	0.485518	0.048342
C21	0.3638	8*b*	0.375000	0.375000	0.375000
H22	0.0152	192*i*	0.339163	0.766400	0.512698
H23	0.0152	192*i*	0.399863	0.692000	0.491198
H24	0.0152	192*i*	0.308763	0.665700	0.515298
H25	0.0152	192*i*	0.308763	0.478600	0.536798
C26	0.7299	16*c*	0	0	0
H27	0.0612	192*i*	−0.019228	0.084817	−0.010691
H28	0.0612	192*i*	0.041472	0.010417	−0.032191
H29	0.0612	192*i*	−0.049628	−0.015883	−0.008091
H30	0.0612	192*i*	−0.049628	0.036717	0.013409

bon atoms are 12 (0.7299/0.0612) times those of the hydrogen atoms in the S cages, which are equal to 192/16. Consequently, there are four hydrogen and one carbon in a methane molecule.

The distribution of methane and propane over hydrate cages is an important but controversial property of synthesized methane-propane hydrate [36–39]. For example, Ripmeester and Ratcliffe [38] synthesized sII hydrate using a gas mixture of 70% methane and 30% propane and found that methane occupied the cages of both types. Susilo *et al.* [37] predicted through a theoretical thermodynamic model that the filling rates of methane were 72% and 25% in the S and L cages, respectively, at 273 K with an initial propane concentration of 1% in the feed gas. However, by refining the neutron results, Hoshikawa *et al.* [36] found that the filling rate of propane in L cages was 100% (the methane: propane ratio in the feed gas was 2:1). Since the methane concentration in the feed gas used in our experiments is much higher than that in previously used feed gas, leading to a higher probability of methane occupying the L cages. The L cages are occupied by both methane and propane, while the S cages are occupied only by methane. This also confirms the thermodynamic model proposed by Susilo *et al.* [37]. As naturally occurring gas hydrates contain complex gas compositions with methane as the main gas, their L cages are not occupied by a single gas but instead by multiple gases [40,41]. Therefore, our results have important practical significance for further exploration of hydrate properties.

As listed in Table 2, the filling rates of methane and propane in the L cages of methane-propane hydrate are 36.38% and 59.28%, respectively, suggesting the almost complete filling rate of the L cages. This is essential for the hydrate stability. However, the gas occupancy of the S cage in the hydrate is only 72.99%, far less than 100%. Therefore, some empty cages exist in hydrate especially the small cages, as shown schematically in Fig. 3(b). This is a normal phenomenon in gas hydrates, which are known to be non-stoichiometric and have partially occupied cages [42–45].

As learned from the cage occupancies of methane and propane, the content of propane in the hydrate is ~25%, approximately 25 times its initial content in the feed gas (~1%), indicating the composition of gas in hydrate is much different from initial feed gas. This result is similar to that obtained by Medvedev *et al.* [46], who found that sII gas hydrate synthesized with 95.7% (mol) methane and 4.3% (mol) propane at 3 MPa contained 36.3% (mol) propane. The preferential enclathration of propane in gas hydrate may be attributed to the higher stability of propane in the L cage.

3.2. Pressure-Temperature (P-T) equilibrium curve of methane-propane hydrate

To investigate the role of propane in the formation of mixed gas hydrate and the preferential enclathration of propane in hydrate, the HLV equilibrium curves of pure methane hydrate (red circles in Fig. 4) and methane-propane deuterated hydrate (black rhombuses in Fig. 4) are determined. The HLV equilibrium curve of methane-propane hydrate with a constant mole ratio (methane: propane = 99:1) is also calculated by CSMHYD program (olive solid

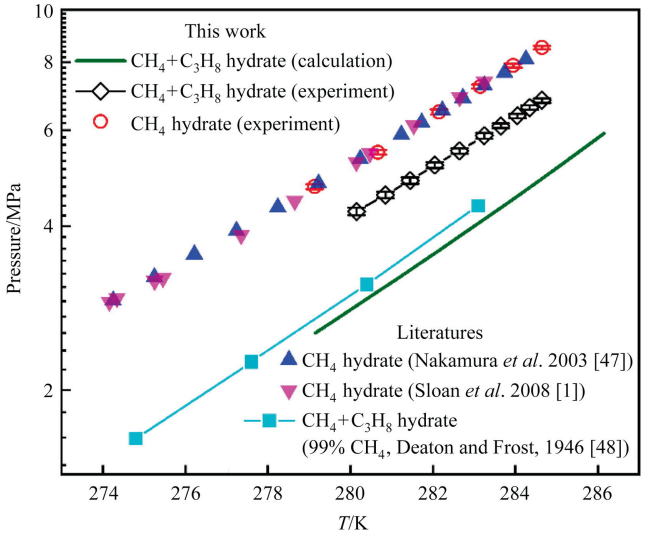

Fig. 4. *P-T* equilibrium curves of methane hydrate and methane-propane hydrate synthesized from a gas mixture with an initial content of 1% (mol) propane. Red circles and black rhombuses represent the methane hydrate and methane-propane deuterated hydrate obtained experimentally in our work, respectively. Olive solid line and cyan solid squares represent the methane-propane hydrate calculated by CSMHYD program in this work and methane-propane deuterated hydrate in literature [48], both of which have constant mole ratios (methane: propane = 99:1). Blue and magenta triangles represent methane hydrate in literatures [1,47].

line in Fig. 4). It can be observed that the phase equilibrium curve of methane hydrate is consistent with the data in the literature [1,47] (blue and magenta triangles in Fig. 4), indicating that our method is reliable. The calculated phase equilibrium curve of methane-propane hydrate is slightly different from the experimental data in literature [48] (cyan solid squares in Fig. 4), but the error (less than 7%) is within the range of experimental accuracy.

The equilibrium pressures of the deuterated hydrate synthesized by the mixed gas with an initial concentration of 1% (mol) propane and 99% (mol) methane are between the equilibrium pressures of methane hydrate and the ones of the hydrate formed with the constant gas composition (calculated values). This demonstrates that the presence of propane can stabilize hydrate, despite its low concentration. The stabilizing effect of propane makes its preferential enclathration in hydrate formation, and the propane in the feed gas decreases rapidly (far below 1% (mol)) and accumulates in the hydrate phase. In the process of equilibrium points measurements, even propane can increase in gas phase to some extent caused by the decomposition of hydrate, its concentration is still well less than 1% (mol). Studies have shown that at low propane concentration, the stability of hydrate is very sensitive to propane concentration and a slight decrease of propane concentration in the gas phase can significantly reduce the stability of the hydrate [37,49]. Therefore, the formed mixed gas hydrate in our experiments is less stable than that of the hydrate synthesized from a constant gas mixture, with a stability between those of methane hydrate and the calculated methane-propane hydrate. The slope of equilibrium line of methane-propane mixed gas hydrate (0.047) is almost parallel to that of methane hydrate (0.046), consistent with the results of Holder *et al.* [50]. However, there is a very slight difference between the slope obtained from experiment (0.047) and the calculated one (0.052), probably due to the different gas composition in hydrate phase and the uncertainty of theoretical simulation.

Table 3
Binding energy of individual methane and propane molecules in different water cages from DFT-D calculations and dispersion correction. S and L stand for small and large water cages, respectively

	sI-S/kJ·mol^{-1}	sI-L/kJ·mol^{-1}	sII-S/kJ·mol^{-1}	sII-L/kJ·mol^{-1}
CH_4	−33.89	−22.09	−36.86	−14.98
C_3H_8	−9.12	−34.06	−19.96	−55.27

3.3. Binding energy and microscopic growth kinetics of methane-propane hydrate

Limited by the experimental methods, only the results after hydrate formation are analysed. Although it can be seen that a small amount of propane plays an important role in determining the crystal structure of hydrate, its specific role in microscopic formation process of sII hydrate is still not clear. Therefore, simulation calculations are combined with experiment to explore the mechanism of low-content propane-induced sII structural formation of the gas hydrate. First, DFT calculation is employed to determine the binding preference of gas molecules to hydrate cages. As shown in Table 3, the binding energy of the methane in the S cages is significantly higher than that in the L cages for both sI and sII hydrates, indicative of the strong preference of methane for the S cages. Similarly, the much larger binding energy of propane in the L cages reveal that propane is with a strong preference for the L cages in hydrates. Further, the binding energies of methane in S cages (−36.86 kJ·mol^{-1}) and propane in L cages (−55.27 kJ·mol^{-1}) in sII hydrate are higher than those in sI hydrate (methane in S cages: −33.89 kJ·mol^{-1}; propane in L cages: −34.06 kJ·mol^{-1}), confirming the higher stability of sII hydrate over sI hydrate in the mixed feed gas. The highest binding energy of propane in L cages suggests that the interaction between propane and L cages is crucial to stabilize hydrate lattice. The calculated results consistent with the trend from the previous calculation work [16] can well explain the formation of sII hydrate and the preferential enclathration of propane in terms of thermodynamic stability. Simultaneously, although methane is with a lower binding energy for the L cages, its high content in the feed gas still leads to some methane-occupying L cages in sII hydrate.

In addition to the binding energy calculation, to further investigate the molecular mechanism of methane-propane hydrate formation, the growth kinetics of the sI/sII hydrates is also investigated for the first time with MD simulation, which uses a

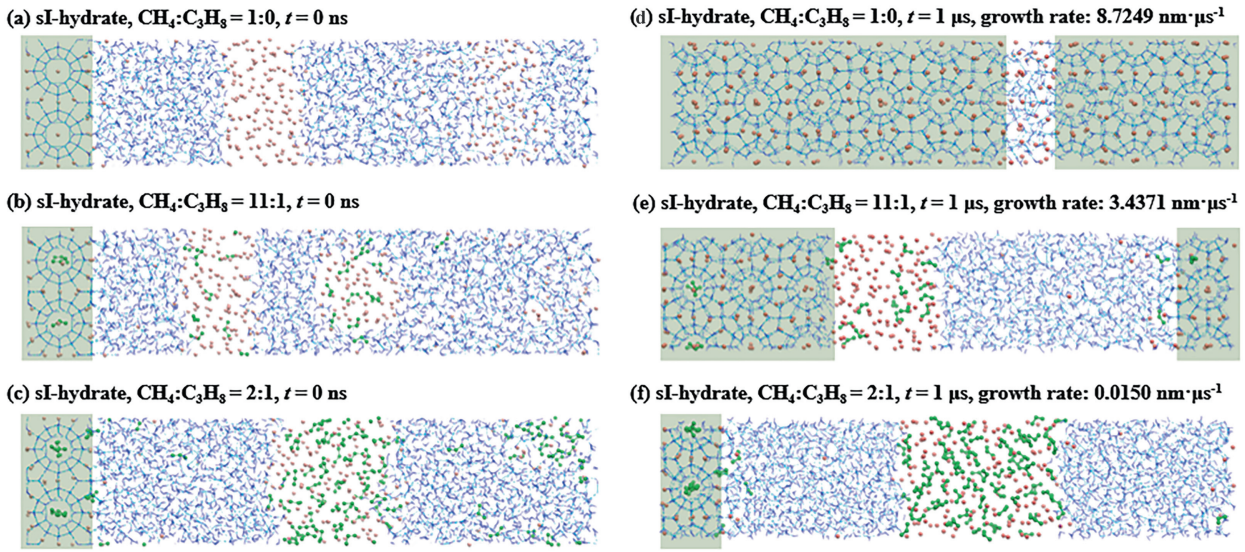

Fig. 5. Snapshots of MD simulation of sI hydrate growth from gases with different methane/propane ratios at the beginning and end of the simulation (simulation condition: 80 MPa, 260 K and 1 μs). Green balls represent carbon atoms in propane and pink balls represent carbon atoms in methane. Blue solid lines represent water cages and cyan dotted lines represent H-bonds.

direct coexistence system of the solid–liquid interfaces [51] with pure methane gas and mixed gases (methane: propane ratios are 1:0, 11:1, and 2:1). As referring to the melting points of hydrates (T_m = 271−279 K, with an error range of ~2 K), 260 K (slightly below T_m) is selected as the simulation temperature for all systems to predict the hydrate growth rates. The snapshots of final hydrate growth rates are shown in Fig. 5 and Fig. 6 for hydrate/solution coexisting systems with different initial methane/propane ratios (at 80 MPa, 260 K, and 1 μs), and more details can be found in Fig. S1 and Fig. S2 from Supplementary Material, depicting the structures intercepted at different simulation times for different crystals.

In Fig. 7, the formation rates of hydrates from the gases with different methane: propane ratios are displayed over time based on the MD simulation results. It can be seen that, the growth rates of sI are significantly affected by the propane content (Fig. 7(a)), decreasing greatly with higher propane content; by contrast, the growth rates of sII remains nearly unchanged (Fig. 7(b)). This implies that propane inhibits the growth of sI hydrate, but is with a negligible effect on the growth of sII hydrate. Thus, during the formation of methane-propane hydrate, the presence of propane is detrimental to the growth of sI hydrate and beneficial to the growth of sII hydrate. It can be speculated that a mixture of sI/sII hydrates might have formed in the initial stage. However, in the subsequent growth process, the growth of sI hydrate is strongly inhibited by propane, while the formation of sII hydrate can go as it is. As the result, the growth rate of sI hydrate is limited, and the formed sI hydrate gradually transforms into the thermodynamically preferred phase (sII). Consequently, when the reaction is completed, sI hydrate is nearly disappeared, and only sII hydrate is observed.

Finally, the occupancies of methane and propane over the cages of the newly formed hydrate are examined. In Table 4, it is notable that the S cages are only occupied by methane molecules as they are not large enough to hold a propane molecule, while the L cages are occupied by both methane and propane. With increasing pro-

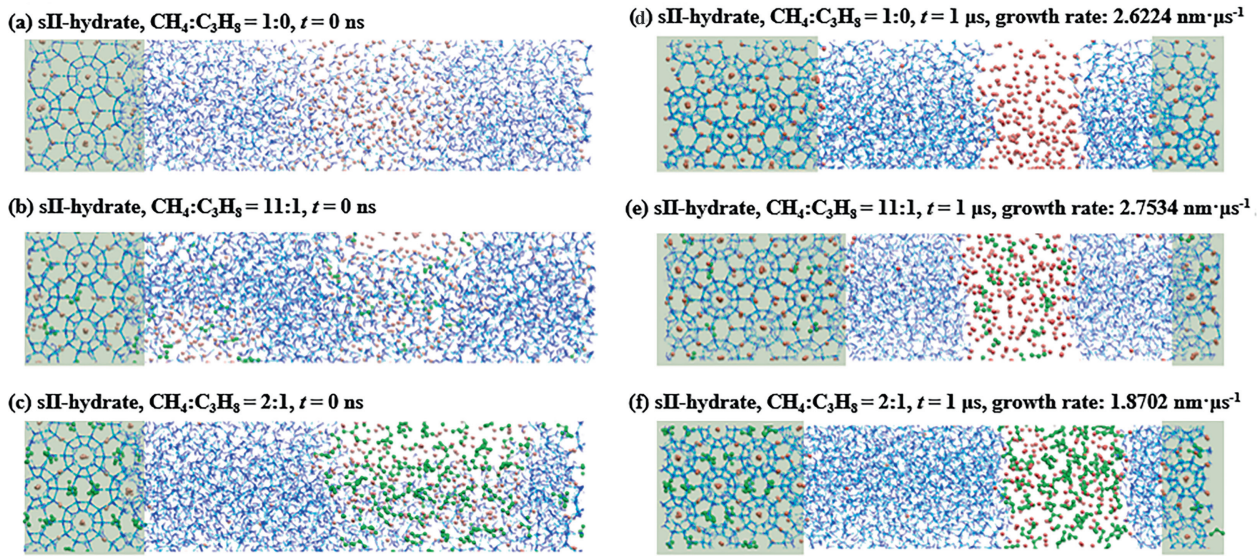

Fig. 6. Snapshots of MD simulation of sII hydrate growth from gases with different methane/propane ratios at the beginning and end of the simulation (simulation condition: 80 MPa, 260 K and 1 μs). Green balls represent carbon atoms in propane and pink balls represent carbon atoms in methane. Blue solid lines represent water cages and cyan dotted lines represent H-bonds.

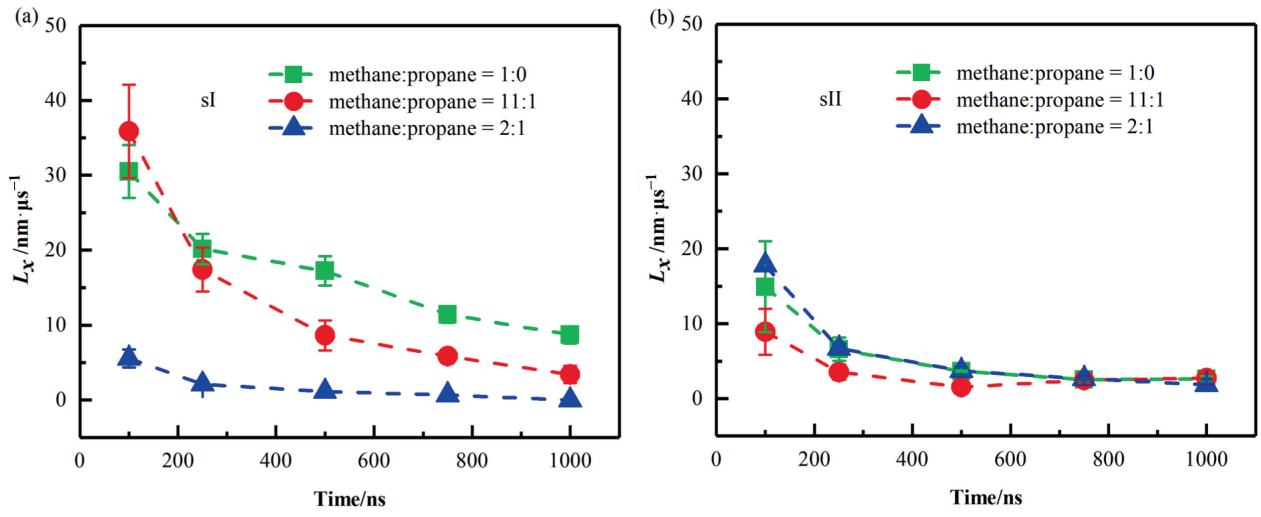

Fig. 7. Growth rates of hydrates formed from the gases with different methane: propane ratios at 80 MPa, 260 K and in different simulation times. L_x represents the growth rates of hydrates. The green, red and blue dotted lines represent the methane-to-propane ratios of 1:0, 11:1 and 2:1, respectively. (a) sI and (b) sII.

Table 4
Cage occupancies under different methane-propane gas ratios at 80 MPa, 260 K, and 1 μs (cage occupancies of propane are shown in parentheses)

	sI-Core		sII-Core	
	5^{12}	$5^{12}6^2$	5^{12}	$5^{12}6^4$
1:0	0.922	0.896	0.990	0.929
11:1	0.875	0.861 (0.084)	0.760	0.708 (0.115)
2:1	—	—	0.651	0.125 (0.552)

Note: No calculation of occupancies for methane in sI cages.

pane concentration, the filling rate of methane in L cages decreases and that of propane increases. The trends of regarding cage occupancies obtained by simulation are consistent with the experimental observation (More details can be found in Fig. S3 and Fig. S4 in Supplementary Material).

4. Conclusions

In this study, high-resolution NPD and theoretical simulations are applied to study the properties and micro-formation mechanism of mixed methane-propane hydrate. The rietveld analyses show that the structure of hydrate formed from methane-propane gas mixture initially containing 1% (mol) propane is sII. The L cages are occupied by methane and propane molecules and the filling rates are 36.38% and 59.28%, respectively. The S cages are occupied by methane and the filling rate is 72.99%. The HLV results show that the addition of propane can have hydrate formed at relatively low-pressure conditions. According to DFT calculations, the binding energy of propane in sII-L cages is greater and the interaction between propane and sII-L cages is stronger, revealing why propane can stabilize hydrates better from a thermodynamic point of view. As the binding energy is much higher for propane in sII-L cages than that in sI-L cages and the binding energy of methane in sII-S cages is close to that in the sI-S cages, the formation of sII hydrate is thermodynamically preferred. Based on the growth rates under different propane contents in MD simulations, propane is found with strong effect inhibiting the formation of sI hydrate. It can be speculated that even if sI and sII hydrates coexist in the initial stage of hydrate formation but, the growth rates of sI hydrate are strongly inhibited and the formed sI hydrates might have gradually transformed into the more stable sII hydrate with reaction progress. Consequently, sII hydrate becomes dominate. With a comprehensive approach of experiment and theoretical simulation, the role of low-concentration propane in the properties (hydrate structure, gas distribution over hydrate cages and thermodynamic stability) and formation of sII mixed gas hydrate is investigated. Thus, the properties of natural sII hydrate can be further understood and a possible microscopic formation mechanism of natural sII hydrate has been proposed. The results obtained can benefit the study of reservoir formation of NGH and optimizing the conditions for natural gas storage and transportation in the form of hydrate.

CRediT Authorship Contribution Statement

Sanya Du: Investigation, Data curation, Writing – original draft. **Xiaomin Han:** Formal analysis, Data curation. **Wenjiu Cai:** Investigation. **Jinlong Zhu:** Funding acquisition. **Xiaobai Ma:** Investigation, Resources, Funding acquisition. **Songbai Han:** Resources. **Dongfeng Chen:** Resources. **Yusheng Zhao:** Writing – review & editing. **Hui Li:** Methodology, Software, Resources, Supervision, Funding acquisition. **Hailong Lu:** Resources, Conceptualization, Funding acquisition. **Xiaohui Yu:** Conceptualization, Resources, Supervision, Funding acquisition.

Declaration of Competing Interest

The authors declare that they have no known competing financial interests or personal relationships that could have appeared to influence the work reported in this paper.

Acknowledgements

This work is supported by the National Key Research and Development Program of China (2016YFA0401503 and 2018YFA0305700), the National Natural Science Foundation of China (11575288, 91934303, 21935001 and 11775011), the Strategic Priority Research Program and Key Research Program of Frontier Sciences of the Chinese Academy of Sciences (XDB33000000, XDB25000000 and QYZDBSSW-SLH013), the Youth Innovation Promotion Association of the Chinese Academy of Sciences (Y202003), the China Geological Survey (DD20190234), and the Scientific Instrument Developing Project (ZDKYYQ20170001) of the Chinese Academy of Sciences.

Supplementary Material

Supplementary data to this article can be found online at https://doi.org/10.1016/j.cjche.2022.10.014.

References

[1] E.D. Sloan, C.A. Koh, Clathrate Hydrates of Natural Gases, third ed., CRC Press, Boca Raton, 2008.
[2] K. Wallmann, E. Pinero, E. Burwicz, M. Haeckel, C. Hensen, A. Dale, L. Ruepke, The global inventory of methane hydrate in marine sediments: A theoretical approach, *Energies* 5 (7) (2012) 2449–2498.
[3] A.A. Swaranjit Singh, Techniques for exploitation of gas hydrate (clathrates) an untapped resource of methane gas, *J. Microb. Biochem. Technol.* 7 (2) (2015) 108–111.
[4] K.A. Kvenvolden, Gas hydrates-geological perspective and global change, *Rev. Geophys.* 31 (2) (1993) 173–187.
[5] Z.R. Chong, S.H.B. Yang, P. Babu, P. Linga, X.S. Li, Review of natural gas hydrates as an energy resource: Prospects and challenges, *Appl. Energy* 162 (2016) 1633–1652.
[6] Y.D. Cui, C. Lu, M.T. Wu, Y. Peng, Y.B. Yao, W.J. Luo, Review of exploration and production technology of natural gas hydrate, *Adv. Geo-Energy Res.* 2 (1) (2018) 53–62.
[7] P. Englezos, J.D. Lee, Gas hydrates: a cleaner source of energy and opportunity for innovative technologies, *Korean J. Chem. Eng.* 22 (5) (2005) 671–681.
[8] H. Liu, S.Y. Zhan, P. Guo, S.S. Fan, S.L. Zhang, Understanding the characteristic of methane hydrate equilibrium in materials and its potential application, *Chem. Eng. J.* 349 (2018) 775–781.
[9] D.L. Katz, D. Cornell, R. Kobayashi, F.H. Poettmann, J.A. Vary, J.R. Elenblass, C.F. Weinaug, Handbook of Natural Gas Engineering, McGraw-Hill, New York, 1959.
[10] E.M. Hendriks, B. Edmonds, R.A.S. Moorwood, R. Szczepanski, Hydrate structure stability in simple and mixed hydrates, *Fluid Phase Equilibria* 117 (1–2) (1996) 193–200.
[11] S. Subramanian, R.A. Kini, S.F. Dec, E.D. Sloan, Evidence of structure II hydrate formation from methane + ethane mixtures, *Chem. Eng. Sci.* 55 (11) (2000) 1981–1999.
[12] J.L. Thakore, G.D. Holder, Solid vapor azeotropes in hydrate-forming systems, *Ind. Eng. Chem. Res.* 26 (3) (1987) 462–469.
[13] C.A. Koh, E.D. Sloan, A.K. Sum, D.T. Wu, Fundamentals and applications of gas hydrates, *Annu. Rev. Chem. Biomol. Eng.* 2 (2011) 237–257.
[14] K.C. Hester, Z. Huo, A.L. Ballard, C.A. Koh, K.T. Miller, E.D. Sloan, Thermal expansivity for sI and sII clathrate hydrates, *J. Phys. Chem. B* 111 (30) (2007) 8830–8835.
[15] H.S. Truong-Lam, S. Seo, S. Kim, Y. Seo, J.D. Lee, *In situ* Raman study of the formation and dissociation kinetics of methane and methane/propane hydrates, *Energy Fuels* 34 (5) (2020) 6288–6297.
[16] Y. Liu, L. Ojamäe, C-C stretching Raman spectra and stabilities of hydrocarbon molecules in natural gas hydrates: A quantum chemical study, *J. Phys. Chem. A* 118 (49) (2014) 11641–11651.
[17] T. Uchida, I.Y. Ikeda, S. Takeya, Y. Kamata, R. Ohmura, J. Nagao, O.Y. Zatsepina, B.A. Buffett, Kinetics and stability of CH_4-CO_2 mixed gas hydrates during formation and long-term storage, *ChemPhysChem* 6 (4) (2005) 646–654.
[18] S.Y. Lee, E. McGregor, G.D. Holder, Experimental study of hydrate crystal growth from methane, carbon dioxide, and methane + propane mixtures, *Energy Fuels* 12 (2) (1998) 212–215.

[19] J. Hutter, M. Iannuzzi, F. Schiffmann, J. VandeVondele, cp2k: Atomistic simulations of condensed matter systems, *Wiley Interdiscip. Rev. Comput. Mol. Sci.* 4 (1) (2014) 15–25.
[20] C. Lee, W. Yang, R.G. Parr, Development of the Colle-Salvetti correlation-energy formula into a functional of the electron density, *Phys. Rev. B Condens. Matter* 37 (2) (1988) 785–789.
[21] A.D. Becke, Density-functional exchange-energy approximation with correct asymptotic behavior, *Phys. Rev. A Gen. Phys.* 38 (6) (1988) 3098–3100.
[22] S. Grimme, J. Antony, S. Ehrlich, H. Krieg, A consistent and accurate *ab initio* parametrization of density functional dispersion correction (DFT-D) for the 94 elements H-Pu, *J. Chem. Phys.* 132 (15) (2010) 154104.
[23] S. Goedecker, M. Teter, J. Hutter, Separable dual-space Gaussian pseudopotentials, *Phys. Rev. B Condens. Matter.* 54 (3) (1996) 1703–1710.
[24] C. Hartwigsen, S. Goedecker, J. Hutter, Relativistic separable dual-space Gaussian pseudopotentials from H to Rn, *Phys. Rev. B* 58 (7) (1998) 3641–3662.
[25] H.J.C. Berendsen, D. van der Spoel, R. van Drunen, GROMACS: A message-passing parallel molecular dynamics implementation, *Comput. Phys. Commun.* 91 (1–3) (1995) 43–56.
[26] H.W. Horn, W.C. Swope, J.W. Pitera, J.D. Madura, T.J. Dick, G.L. Hura, T. Head-Gordon, Development of an improved four-site water model for biomolecular simulations: TIP4P-Ew, *J. Chem. Phys.* 120 (20) (2004) 9665–9678.
[27] W.L. Jorgensen, D.S. Maxwell, J. Tirado-Rives, Development and testing of the OPLS all-atom force field on conformational energetics and properties of organic liquids, *J. Am. Chem. Soc.* 118 (45) (1996) 11225–11236.
[28] D.J. Evans, B.L. Holian, The nose–hoover thermostat, *J. Chem. Phys.* 83 (8) (1985) 4069–4074.
[29] S. Melchionna, G. Ciccotti, B.L. Holian, Hoover *NPT* dynamics for systems varying in shape and size, *Mol. Phys.* 78 (3) (1993) 533–544.
[30] R.K. McMullan, G.A. Jeffrey, Polyhedral clathrate hydrates. IX. Structure of ethylene oxide hydrate, *J. Chem. Phys.* 42 (8) (1965) 2725–2732.
[31] A. Falenty, T.C. Hansen, W.F. Kuhs, Formation and properties of ice XVI obtained by emptying a type sII clathrate hydrate, *Nature* 516 (7530) (2014) 231–233.
[32] W. Cai, H. Lu, X. Huang, Experimental investigations about the effect of trace amount of propane on the formation of mixed hydrates of methane and propane, AGU Fall Meeting Abstracts, San Francisco (2016).
[33] T. Uchida, M. Moriwaki, S. Takeya, I.Y. Ikeda, R. Ohmura, J. Nagao, H. Minagawa, T. Ebinuma, H. Narita, K. Gohara, S. Mae, Two-step formation of methane-propane mixed gas hydrates in a batch-type reactor, *AIChE J.* 50 (2) (2004) 518–523.
[34] J.M. Schicks, R. Naumann, J. Erzinger, K.C. Hester, C.A. Koh, E.D. Sloan, Phase transitions in mixed gas hydrates: Experimental observations versus calculated data, *J. Phys. Chem. B* 110 (23) (2006) 11468–11474.
[35] C.J. Rawn, A.J. Rondinone, B.C. Chakoumakos, S. Circone, L.A. Stern, S.H. Kirby, Y. Ishii, Neutron powder diffraction studies as a function of temperature of structure II hydrate formed from propane, *Can. J. Phys.* 81 (1–2) (2003) 431–438.
[36] A. Hoshikawa, T. Matsukawa, T. Ishigaki, Evaluation of filling rate of methane in methane-propane hydrate by neutron powder diffraction, *Phys. B Condens. Matter* 551 (2018) 274–277.
[37] R. Susilo, S. Alavi, J. Ripmeester, P. Englezos, Tuning methane content in gas hydrates *via* thermodynamic modeling and molecular dynamics simulation, *Fluid Phase Equilibria* 263 (1) (2008) 6–17.
[38] J.A. Ripmeester, C.I. Ratcliffe, Low-temperature cross-polarization/magic angle spinning carbon-13 NMR of solid methane hydrates: structure, cage occupancy, and hydration number, *J. Phys. Chem.* 92 (2) (1988) 337–339.
[39] A.K. Sum, R.C. Burruss, E.D. Sloan, Measurement of clathrate hydrates *via* Raman spectroscopy, *J. Phys. Chem. B* 101 (38) (1997) 7371–7377.
[40] H.L. Lu, Y.T. Seo, J.W. Lee, I. Moudrakovski, J.A. Ripmeester, N.R. Chapman, R.B. Coffin, G. Gardner, J. Pohlman, Complex gas hydrate from the Cascadia margin, *Nature* 445 (7125) (2007) 303–306.
[41] C.L. Liu, Q.G. Meng, X.L. He, C.F. Li, Y.G. Ye, Z.Q. Lu, Y.H. Zhu, Y.H. Li, J.Q. Liang, Comparison of the characteristics for natural gas hydrate recovered from marine and terrestrial areas in China, *J. Geochem. Explor.* 152 (2015) 67–74.
[42] A.G. Aregbe, Gas hydrate—properties, formation and benefits, *Open J. Yangtze Oil Gas* 2 (1) (2017) 27–44.
[43] Z.X. Huo, K. Hester, E.D. Sloan, K.T. Miller, Methane hydrate nonstoichiometry and phase diagram, *AIChE J.* 49 (5) (2003) 1300–1306.
[44] T. Uchida, T. Hirano, T. Ebinuma, H. Narita, K. Gohara, S. Mae, R. Matsumoto, Raman spectroscopic determination of hydration number of methane hydrates, *AIChE J.* 45 (12) (1999) 2641–2645.
[45] J. Vatamanu, P.G. Kusalik, Molecular insights into the heterogeneous crystal growth of sI methane hydrate, *J. Phys. Chem. B* 110 (32) (2006) 15896–15904.
[46] V.I. Medvedev, P.A. Gushchin, V.S. Yakushev, A.P. Semenov, Study of the effect of the degree of overcooling during the formation of hydrates of a methane−propane gas mixture on the equilibrium conditions of their decomposition, *Chem. Tech. Fuels Oil* 51 (5) (2015) 470–479.
[47] T. Nakamura, T. Makino, T. Sugahara, K. Ohgaki, Stability boundaries of gas hydrates helped by methane—structure-H hydrates of methylcyclohexane and *cis*-1, 2-dimethylcyclohexane, *Chem. Eng. Sci.* 58 (2) (2003) 269–273.
[48] E. Frost, W.M. Deaton, Gas hydrate composition and equilibrium data [Direct and calculated measurements are in close agreement; CO_2, CH_4, C_2H_6, C_3H_8 used], *Oil Gas J* 45 (1946) 170–178.
[49] C. Smith, D. Pack, A. Barifcani, Propane, *n*-butane and *i*-butane stabilization effects on methane gas hydrates, *J. Chem. Thermodyn.* 115 (2017) 293–301.
[50] G.D. Holder, P.F. Angert, V.T. John, S. Yen, A thermodynamic evaluation of thermal recovery of gas from hydrates in the earth (includes associated papers 11863 and 11924), *J. Pet. Technol.* 34 (05) (1982) 1127–1132.
[51] R. García Fernández, J.L. Abascal, C. Vega, The melting point of ice Ih for common water models calculated from direct coexistence of the solid-liquid interface, *J. Chem. Phys.* 124 (14) (2006) 144506.